JOURNAL OF SOLID STATE CHEMISTRY 49, 43–50 (1983)

Photoelectronic Properties of Cu_3PS_4 and Cu_3PS_3Se Single Crystals

J. V. MARZIK, A. K. HSIEH,[1] K. DWIGHT, AND A. WOLD[2]

Department of Chemistry, Brown University, Providence, Rhode Island 02912

Received February 21, 1983; in revised form April 4, 1983

Single crystals of Cu_3PS_4 and Cu_3PS_3Se grown by chemical vapor transport were shown to be diamagnetic p-type semiconductors. Electrical measurements showed room temperature resistivities ranging from 1 to 5 ohm-cm and carrier concentrations of 10^{17} cm^{-3}. Both materials were shown to be active as cathodes for the photoelectrolysis of water. Spectral response measurements show that substitution of selenium for sulfur lowers the optical band gap from 2.38(5) eV for Cu_3PS_4 to 2.06(4) eV for Cu_3PS_3Se.

Introduction

One of the first solid-state photovoltaic systems studied is the copper sulfide/cadmium sulfide solar cell (*1*). The composition of copper sulfide in this cell is very close to Cu_2S (*2*). This suggests that copper(I) is a photoactive center and that semiconductors containing copper(I) should be investigated as possible electrodes in photoelectrochemical cells.

The application of semiconductor electrodes in the construction of photoelectrolysis, photovoltaic, and photocatalytic cells has been extensively investigated in recent years. There are several reviews of these studies (*3–5*). Aqueous photoelectrochemical cells based on p-type Cu_2O have been described (*6*); however, the p-Cu_2O cathode was found to be unstable. The photoelectrochemical behavior of p-Cu_2O has also been investigated in nonaqueous systems (*7*), and the material was found to be stable but had low optical-to-electrical energy conversion efficiencies. $CuInS_2$, a nonoxide semiconductor, has also been investigated as a photoelectrode (*8, 9*) and shows reasonably good efficiency and long term stability in aqueous polysulfide solutions.

Recent work in this laboratory (*10*) showing PdPSe to be a photoactive n-type semiconductor has initiated the investigation of other transition metal V-VI semiconductors as possible photoelectrodes. Single crystal growth of Cu_3PS_4 was first reported by Nitsche and Wild (*11*), and the structure of the isostructural Cu_3PSe_4 was determined by Garin and Parthé (*12*) and refined by Toffoli *et al.* (*13*). Cu_3PS_4 and Cu_3PSe_4 are isostructural to the mineral enargite (Cu_3AsS_4), a wurtzite-related structure type in which all atoms are in tetrahedral coordination with phosphorus occupying ordered cation positions. Although detailed studies of the properties of these materials have not been reported, it was thought that these

[1] Department of Chemistry, National University of Singapore, Kent Ridge, Singapore.

[2] To whom all correspondence should be addressed.

0022-4596/83 $3.00

copper(I)-containing materials would be p-type semiconductors and possible photoelectrodes. Furthermore, since Cu_3PS_4 and Cu_3PSe_4 are isostructural, solid solutions of the two compounds should be possible.

Thus, it was of interest to synthesize large single crystals of members of the system $Cu_3PS_{4-x}Se_x$ and to investigate their magnetic, electrical, and photoelectronic properties as functions of composition. The effect of anion substitution on the electronic and photoelectronic properties has previously been investigated in the oxyfluorides $TiO_{2-x}F_x$ (*14*). The substitution of fluorine into TiO_2 was found to enhance the photoresponse and extend it to longer wavelengths. In general, anion substitution is more facile in pnictides and chalcogenides than in oxides. Thus, the substitution of Se for S in Cu_3PS_4 suggests a means of manipulating the electrical properties of the system, perhaps leading to improved photoelectronic properties.

Experimental

Synthesis. Single crystals of Cu_3PS_4, Cu_3PS_3Se, and Cu_3PSe_4 were synthesized by chemical vapor transport using both iodine and bromine. Both transport agents resulted in crystals of identical structural and electrical properties. Experiments using bromine generally resulted in larger crystals. Copper (Johnson-Matthey 99.999%) was prereduced at 450°C for 6 hr under 85%/15% Ar/H_2 gas. Phosphorus (Leico 99.999%) was washed with distilled water and dried under vacuum. Selenium (Gallard-Schlesinger 99.999%) and sulfur (Gallard-Schlesinger 99.999%) were freshly sublimed. Transport tubes were prepared with an H-tube filling apparatus as previously described (*15*). Stoichiometric quantities of the elements were added for the growth of Cu_3PS_4 and Cu_3PSe_4. For growth of Cu_3PS_3Se, the charge contained Cu:P:S:Se in a 3:1:2:2 ratio (see Results and Discussion). The transport tube was placed in a three-zone furnace and the charge prereacted for 24 hr at 600°C with the growth zone at 1000°C preventing transport of product. The furnace was then equilibrated at 850°C and programmed over 24–48 hr to give a temperature of 825°C in the charge zone and 775°C in the growth zone. Crystal growth took place in 5–7 days. Cu_3PS_4 formed transparent yellow–brown prisms up to 10 × 2 × 2 mm. Cu_3PS_3Se formed red platelets up to 50 mm^2 and 50 μm thickness. Cu_3PSe_4 formed small (<1 mm) black tetrahedra. Polycrystalline samples were synthesized by the reaction of stoichiometric amounts of the elements in evacuated silica tubes at 750–800°C for 7 days with several intermittent shakings.

X-Ray analysis. X-Ray diffraction patterns of single crystals were obtained using a Gandolfi camera (Blake Industries Model D1100) and Ni-filtered Cu$K\alpha$ radiation. X-Ray diffraction patterns of polycrystalline samples were obtained with a Norelco diffractometer using monochromatic high-intensity Cu$K\alpha_1$ radiation (λ = 1.5405 Å) at a scan rate of 0.25° 2θ/min. Lattice parameters were obtained by least squares refinement of the diffraction data.

Magnetic measurements. Magnetic susceptibility was measured using a Faraday balance (*16*) over the range from liquid nitrogen to room temperature at a field strength of 10.4 kOe. Honda–Owen plots (*17*) were also made, and the absence of any field dependency indicated the absence of ferromagnetic impurities. No corrections were made for core diamagnetism because of the large uncertainty in the magnitude of the corrections relative to the magnitude of the observed susceptibility values.

Electrical measurements. Resistivity and DC Hall effect were measured on single crystals using the van der Pauw technique (*18*). Contacts were made to the crystal with colloidal graphite (Acheson Electro-

Dag) and ohmic behavior was established by measuring current–voltage characteristics. Activation energy of resistivity E_a (defined for semiconductors by $\rho = \rho_0 \exp(E_a/kT)$ where ρ = resistivity, ρ_0 is a constant, T = temperature (K), and k = Boltzmann constant) was determined by measuring ρ as a function of T.

Electrode preparation. Photoelectrodes were prepared by evaporating thin films of gold on the backs of the single crystals of Cu_3PS_4 and Cu_3PS_3Se in order to provide good electrical contact. For mechanical support, the gold face of each crystal was affixed to a disk of platinum foil with a drop of silver paint. The platinum foil was soldered to a platinum wire which was sealed inside a Pyrex tube, and the electrode was rinsed with CCl_4 (Fischer Spectroanalyzed) and air dried. An insulated resin (Miccrostop, Michigan Chrome Chemical Corp.) was applied to the platinum foil and wire so that only the front surface of the crystal was in electrical contact with the electrolyte solution. Electrodes were rinsed with methanol (Fischer Certified Electronic Grade) and air dried before each measurement.

Photoelectrochemical measurements. Photoelectrochemical measurements were carried out with a 150-W xenon lamp, a monochromator (Oriel Model 7240), a glass cell with a quartz window, and a current amplifier as previously described (*14*). A platinized platinum electrode was used as a counter electrode. Potential measurements were made with respect to a saturated calomel electrode (Fischer 13-639-56). For sample current–potential measurements under steady-state conditions, bias was applied via a potentiometer and a voltage follower having a very low output impedance (<0.1 ohm). For cyclic voltammetric measurements, the voltage was driven via a sweep generator and a voltage follower. Voltammograms were recorded on a Hewlett–Packard Model 7035B X-Y recorder. For wavelength dependency measurements, the quantum efficiency was determined by dividing the current through the cell by the incident photon flux, measured with a calibrated Si photodiode.

Analyzed reagent grade chemicals and deionized water (18.3 MΩ) were used in order to minimize impurities in the electrolyte. In general, the electrolyte was 0.1 *M* K_2HPO_4 (pH 9.3). For the sampled current–potential measurements, the electrolyte was continuously bubbled with 85%/15% Ar/H_2 gas which gave a potential of −0.75 V versus SCE at zero bias. Before each cyclic voltammetric measurement, the solution was purged with nitrogen gas.

Results and Discussion

X-Ray analysis shows that members of the system $Cu_3PS_{4-x}Se_x$ have orthorhombic diffraction symmetry. Cell dimensions for both polycrystalline and single crystal samples are listed in Table I. Values obtained for Cu_3PS_4 and Cu_3PSe_4 agree well with those obtained by Garin and Parthé (*12*). Cell dimensions of polycrystalline samples indicate that members of the system are isostructural and follow Végard's law (*19*). Cell dimensions of Cu_3PS_4 single crystals agree well with those of polycrystalline samples. From a Végard plot, using cell pa-

TABLE I

X-RAY DATA FOR THE $Cu_3PS_{4-x}Se_x$ SYSTEM

	a(Å)	b(Å)	c(Å)	V (Å^3)
Cu_3PS_4[a]	7.281(2)	6.294(2)	6.066(2)	278.0(3)
Cu_3PS_3Se[a]	7.395(2)	6.408(2)	6.143(2)	291.1(3)
$Cu_3PS_2Se_2$[a]	7.488(2)	6.499(2)	6.231(2)	303.2(3)
Cu_3PSe_4[a]	7.700(1)	6.700(1)	6.396(2)	330.0(2)
Cu_3PS_4[b]	7.290(6)	6.326(6)	6.040(6)	278.5(8)
Cu_3PS_3Se[b]	7.371(6)	6.421(6)	6.156(6)	291.4(8)

[a] Polycrystalline samples.
[b] Single crystals.

TABLE II

PROPERTIES OF Cu_3PS_4 AND Cu_3PS_3Se SINGLE CRYSTALS

	Cu_3PS_4	Cu_3PS_3Se
Color	Yellow–brown	Red
Resistivity[a] (ohm-cm)	1	4
E_a (eV)	0.06	0.06
Carrier concentration[a] (cm^{-3})	1.8×10^{17}	1.5×10^{17}
Hall mobility[a] ($cm^2\ V^{-1}\ sec^{-1}$)	30	10
Carrier type	p	p
Optical band gap (eV)	2.38	2.06

[a] 298°K.

rameters of polycrystalline samples of various compositions, single crystals grown with equal amounts of sulfur and selenium in the charge were determined to have the composition $Cu_3PS_{2.96\pm0.06}Se_{1.04\pm0.06}$. This is consistent with the observation that Cu_3PS_4 transported more readily than Cu_3PSe_4 under the experimental conditions used.

The electrical properties of Cu_3PS_4 and Cu_3PS_3Se are summarized in Table II. Seebeck and Hall measurements show that both are p-type semiconductors. Magnetic susceptibility measurements indicate that both Cu_3PS_4 and Cu_3PS_3Se are diamagnetic. The absence of a localized moment is consistent with copper existing in the structure as d^{10} Cu(I).

The photoresponses observed for Cu_3PS_4 and Cu_3PS_3Se single crystals from sampled current–potential measurements under steady-state conditions are shown in Fig. 1, where the photocurrents obtained in "white" light are plotted against the potential of the working electrode measured with respect to a saturated calomel electrode (SCE). The p-type materials were used as photocathodes. The onset potential of photocurrent was approximately −0.8 V versus SCE for Cu_3PS_4 and −0.9 V versus SCE for Cu_3PS_3Se at pH 9.3 in 0.1 *M* K_2HPO_4. Maximum photoresponse is greater in Cu_3PS_3Se indicating an enhancement due to the pres-

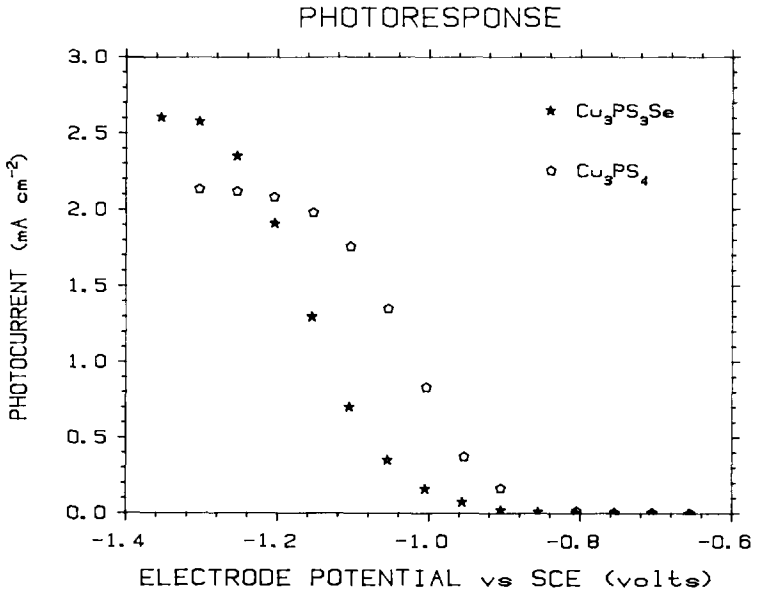

FIG. 1. Variation of photocurrent with electrode potential under "white" xenon arc irradiation of 1.0 W/cm² in 0.1 *M* K_2HPO_4 electrolyte solution.

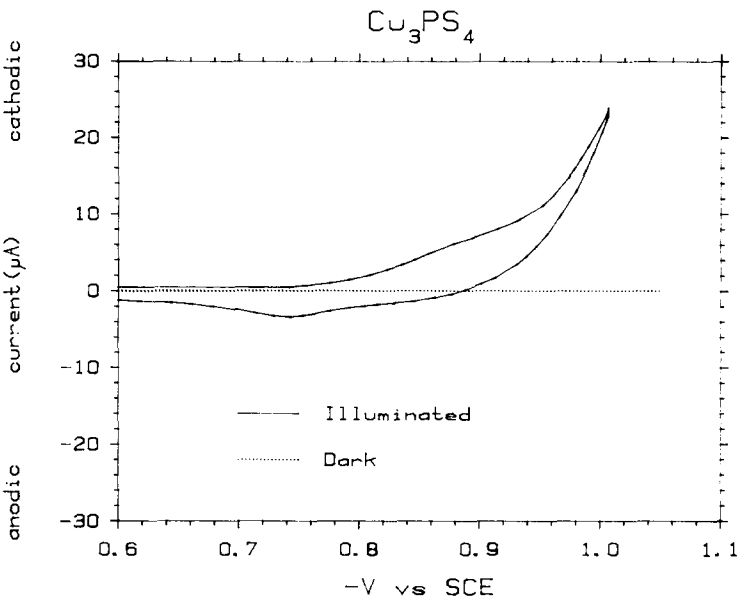

FIG. 2. Cyclic voltammogram in the region of photoresponse under "white" xenon arc irradiation of 1.0 W/cm² in 0.1 *M* K_2HPO_4 at a sweep rate of 25 mV/sec.

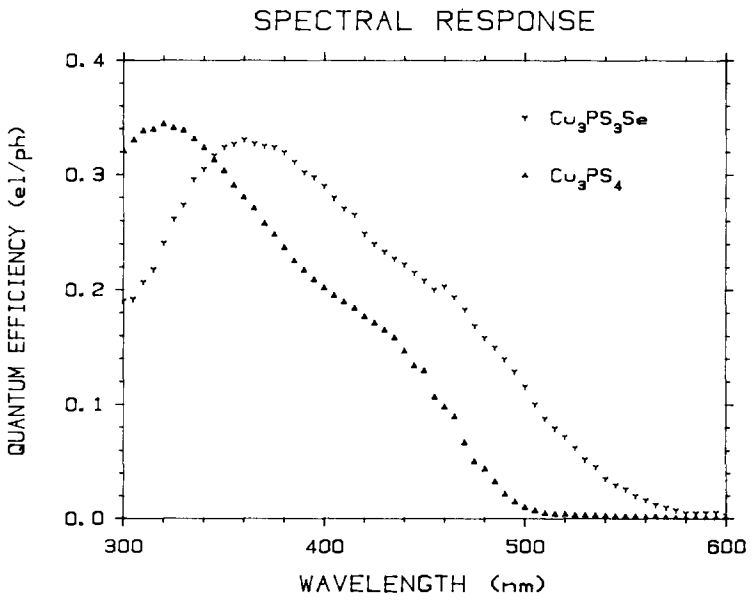

FIG. 3. Spectral variation of the quantum efficiency obtained at an electrode potential of −1.25 V versus SCE in 0.1 *M* K_2HPO_4.

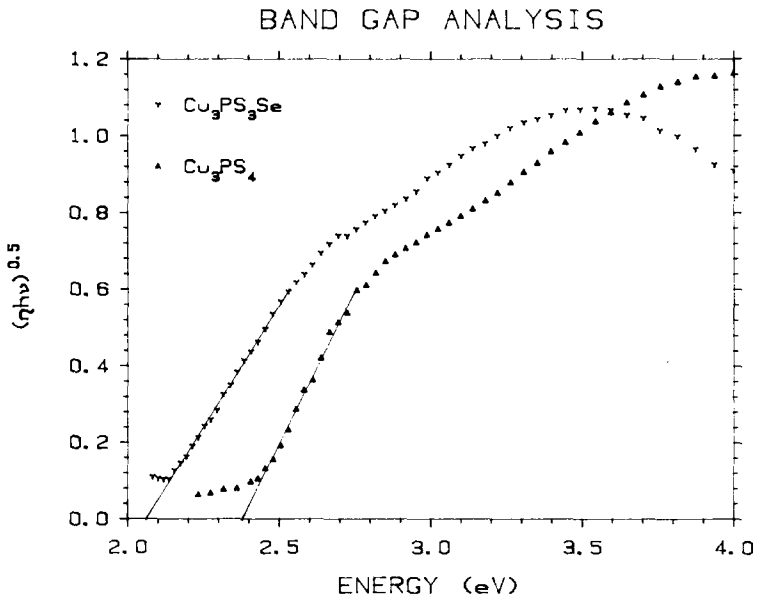

FIG. 4. Indirect band gap analysis for Cu_3PS_4 and Cu_3PS_3Se giving lowest-energy indirect optical band gaps of 2.38(5) eV and 2.06(4), respectively.

ence of Se. However, because of its more negative onset potential, a larger bias was required for Cu_3PS_3Se to reach its maximum photoresponse.

Cathodic dark current was small (0–0.5 mA cm^{-2}) compared to the observed cathodic photocurrent. Cyclic voltammograms of Cu_3PS_4 (see Fig. 2) taken in the region of the photoresponse are consistent with the results from the sampled current–potential measurements. A plot of the onset potential of the photocurrent versus pH from cyclic voltammograms at various pH values follows the expected Nernstian behavior (with a slope of 59 mV/pH unit) predicted for hydrogen reduction at the working electrode. Hence, the photocurrent can be attributed to the reduction of hydrogen ion to hydrogen gas at the semiconductor.

The quantum efficiency η (in electrons/photon) measured at a working electrode potential of -1.25 V versus SCE is plotted versus wavelength in Fig. 3. There is a marked shift of the spectral response toward longer wavelengths upon selenium substitution into Cu_3PS_4. The onset of photocurrent occurs at 510 nm for Cu_3PS_4 and 580 nm for Cu_3PS_3Se. Following the onset, there is a steady increase in η with decreasing wavelength which reaches a maximum at 320 nm for Cu_3PS_4 and 370 nm for Cu_3PS_3Se.

Analysis of the spectral response data can yield values for various energy transitions (*20*). Accordingly, the quantity $(\eta h\nu)^{0.5}$ plotted as a function of photon energy (Fig. 4) yields a lowest energy indirect optical band gap of 2.38(5) eV for Cu_3PS_4 and 2.06(4) eV for Cu_3PS_3Se. Thus, the substitution of Se into Cu_3PS_4 has the effect of lowering the optical band gap. A plot of the spectral response data against the solar spectrum at air mass 1 (Fig. 5) clearly shows an enhancement in the solar region upon selenium substitution.

Experiments under constant illumination (1 W/cm^2) were performed for both Cu_3PS_4 and Cu_3PS_3Se to determine stability. At pH

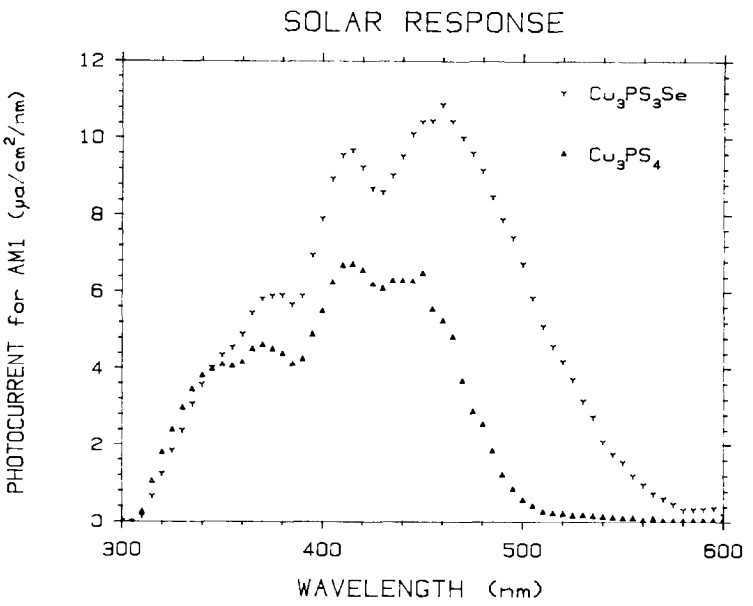

FIG. 5. Solar response for air mass 1 (AM1) calculated from the data presented in Fig. 3.

9.3 in 0.1 *M* K_2HPO_4, the electrode was held at −1.2 V versus SCE. For both electrodes, the photocurrent was observed to decay to 20% of its original value after 3 hr and the electrodes darkened visibly. Although the exact nature of the instability was not determined, it probably involves the reduction of Cu(I) to Cu(0).

Summary and Conclusions

Large single crystals of Cu_3PS_4 and Cu_3PS_3Se have been grown by chemical vapor transport, and several of their properties have been investigated. Both are diamagnetic p-type semiconductors and were found to be photoactive as cathodes for the photoelectrolysis of water. Substitution of Se into Cu_3PS_4 slightly enhances the photoresponse; however, the onset potential of photocurrent is also shifted to a more negative value for Cu_3PS_3Se and a larger bias voltage is required to reach maximum photoresponse. Photoelectronic spectral response measurements show that Se substitution lowers the optical band gap from 2.38 eV for Cu_3PS_4 to 2.06 eV for Cu_3PS_3Se and shifts the photoresponse to longer wavelengths, thus enhancing the activity in the solar region. The materials were found to lack long term stability under constant illumination with the electrolytes used.

It has been shown that it is possible to manipulate the electronic, optical, and photoelectronic properties of a transition metal V–VI semiconductor by means of anion substitution. This suggests the possibility of using other semiconductors of this type as photoelectrodes and the maximization of their photoelectronic properties by anion substitution.

Acknowledgments

The authors thank GTE Laboratories, Inc. of Waltham, Mass., for the support of James V. Marzik. Acknowledgment is also made to the National Science Foundation (DMR-82-03667) for the support of Kirby

Dwight, and to Brown University for the use of its Materials Research Laboratory facilities.

References

1. D. C. Reynolds, G. Leies, L. L. Antes, and R. E. Marburger, *Phys. Rev.* **96,** 533 (1954).
2. T. S. teVelde and J. Dielman, *Philips Res. Rep.* **28,** 573 (1973).
3. A. J. Nozik, *Annu. Rev. Phys. Chem.* **29,** 189 (1978).
4. M. S. Wrighton, *Acc. Chem. Res.* **12,** 303 (1979).
5. A. J. Bard, *Science* **207,** 139 (1980).
6. K. Hauffe and K. Reinhold, *Ber. Bunsenges. Phys. Chem.* **76,** 616 (1972).
7. G. Nagasubramanian, A. S. Gioda, and A. J. Bard, *J. Electrochem. Soc.* **128,** 2158 (1981).
8. M. Robbins, K. J. Bachmann, V. G. Lambrecht, F. A. Thiel, J. Thomson, Jr., R. G. Vadimsky, S. Menezes, A. Heller, and B. Miller, *J. Electrochem. Soc.* **125,** 831 (1978).
9. Y. Mirovsky, D. Cahen, G. Hodes, R. Tenne, and W. Giriat, *Solar Energy Mater.* **4,** 169 (1981).
10. J. V. Marzik, R. Kershaw, K. Dwight, and A. Wold, *J. Solid State Chem.* **44,** 382 (1982).
11. R. Nitsche and P. Wild, *Mater. Res. Bull.* **5,** 419 (1970).
12. J. Garin and E. Parthé, *Acta Crystallogr. Sect. B* **28,** 3672 (1972).
13. P. Toffoli, N. Rodier, and P. Khodadad, *Bull. Soc. Fr. Mineral. Cristallogr.* **99,** 403 (1976).
14. S. N. Subbarao, Y. H. Yun, R. Kershaw, K. Dwight, and A. Wold, *Mater. Res. Bull.* **13,** 1461 (1978).
15. R. Kershaw, M. Vlasse, and A. Wold, *Inorg. Chem.* **6,** 1599 (1967).
16. B. Morris and A. Wold, *Rev. Sci. Instrum.* **39,** 1937 (1968).
17. L. F. Bates, "Modern Magnetism," Cambridge Univ. Press, New York (1961).
18. L. J. van der Pauw, *Philips Res. Rep.* **13,** 1 (1958).
19. H. Krebs, "Fundamentals of Inorganic Crystal Chemistry," McGraw–Hill, London (1968).
20. F. P. Koffyberg, K. Dwight, and A. Wold, *Solid State Commun.* **30,** 433 (1979).